ACS APPLIED MATERIALS & INTERFACES

RESEARCH ARTICLE

www.acsami.org

Platinum Nanoparticle Modified Polyaniline-Functionalized Boron Nitride Nanotubes for Amperometric Glucose Enzyme Biosensor

Jianmin Wu and Longwei Yin*

Key Laboratory for Liquid−Solid Structural Evolution and Processing of Materials, Ministry of Education, School of Materials Science and Engineering, Shandong University, Jinan 250061, People's Republic of China

ABSTRACT: A novel amperometric biosensor based on the BNNTs-Pani-Pt hybrids with Pt nanoparticle homogeneously decorated on polyaniline (Pani)-wrapped boron nitride nanotubes (BNNTs), was developed. It is shown that π interactions take place between BNNTs and polyaniline (Pani) located at N atoms from BNNTs and C atoms from Pani, resulting in the water solubility for the Pani wrapped BNNTs hybrids. The developed glucose biosensor displayed high sensitivity and stability, good reproducibility, anti-interference ability, especially excellent acid stability and heat resistance. The resulted BNNTs-Pani-Pt hybrid amperometric glucose biosensor exhibited a fast response time (within 3 s) and a linear calibration range from 0.01 to 5.5 mM with a high sensitivity and low detection limit of 19.02 mA M^{-1} cm^{-2} and 0.18 μM glucose (S/N = 3). Surprisedly, the relative activity of the GC/BNNTs-Pani-Pt-GOD electrode keeps almost no change in a range from pH 3 to 7. Futhermore, the BNNTs-Pani-Pt hybrid biosensor maintains a high GOD enzymatic activity even at a relatively high temperature of 60 °C. This might be attributed to the effect of electrostatic field and hydrophobia of BNNTs. The unique acid stability and heat resistance of this sensor indicate great promising application in numerous industrial and biotechnological operations involving harsh conditions.

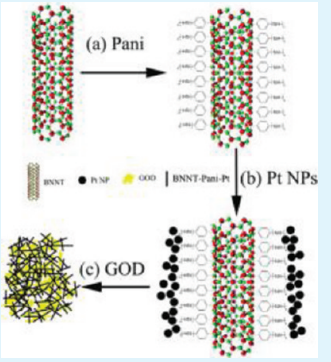

KEYWORDS: boron nitride nanotubes, polyaniline, platinum nanoparticles, glucose biosensor, acid stability, heat resistance

1. INTRODUCTION

Boron nitride nanotubes (BNNTs), a rising wide band gap semiconductor, have been given considerable attention since they were first produced in 1995.[1] To date, BNNTs have the most prospective applications in composite materials,[2,3] luminescent nanomaterials,[4] thermal conductive polymer[5] because of their superb elasticity and strength, high thermal conductivity, high resistance to oxidation, unique luminescence, high surface-to-volume ratio, and so on. So BNNTs are superior for use as catalyst supporters. Actually, carbon nanotubes (CNTs), structurally similar to BNNTs, have been widely used in the field of biosensors.[6,7] There is every reason to believe that BNNTs can be a promising candidate in biosensor applications. However, there are still some developmental challenges to be addressed. One of the major barriers is the insolubility of BNNTs in most solvents, which may greatly limit their application in biosensor systems.[2,8] To improve water solubility of BNNTs, it is necessary to functionalize BNNTs through covalent and/or noncovalent bonding to hydrophilic groups or molecules. Considerable efforts have been devoted toward their solubilization via functionalization and wrapping with molecules such as quinuclidine,[9] amine and phosphine,[10] biomolecule,[11,12] protein,[13] polyaromatic systems,[14] and various polymers such as poly (ethyleneglycol),[15] polyanilines (Pani),[16] poly(*p*-phenylene-ethynylene)s, polythiophene,[17] and polyphenylenevinylenes (PmPV).[2] On the other hand, for the applications in optoelectronic and biological applications for BNNT-related composites, preferable electronic conductivity should be obtained for the functionalized BNNTs.

Polyaniline (Pani), one of the most studied conducting polymers, which has the similar electronic, magnetic, and optical properties to metals, has been extensively studied for many applications including supercapacitors,[18] anticorrosioncoating,[19] light-emitting diodes,[20] conducting molecular wires,[21] sensors,[22] and so forth. What is more, Pani also retains the flexibility and processability of conventional polymers. In biosensor applications, Pani is a perfect matrix for the immobilization of enzyme[23−25] and can act as a mediator to improve signal amplification significantly in enzymatic reaction. On the other hand, Pani also provides an excellent matrix for dispersing noble metals, which expands its usage, and has been used in the fields of catalysts and sensors.[23,26] Zhou et al. reported a glucose sensor based on Pt nanoparticle dispersed nanofibrous Pani, showing an excellent antiinterference, good stability, and reproducibility.[26]

Herein, on the basis of large scale synthesis of BNNTs, the BNNTs were successfully modified and wrapped using polyaniline (Pani) to solve the water solubility. The water solubility of BNNTs paves the way for the following Pt loading. An amperometric biosensor based on the BNNTs-Pani-Pt hybrids with Pt nanoparticle homogeneously decorated on polyaniline (Pani)

Received: July 30, 2011
Accepted: October 20, 2011
Published: October 20, 2011

wrapped boron nitride nanotubes (BNNTs), was developed. The developed glucose biosensor displayed high sensitivity and stability, good reproducibility, anti-interference ability, especially excellent acid stability, and heat resistance. The unique acid stability and heat resistance of this sensor indicate great promising application in numerous industrial and biotechnological operations involving harsh conditions.

2. EXPERIMENTAL SECTION

2.1. Chemicals and Reagents. Glucose oxidase (from *Aspergillus niger*, 200 U mg^{-1}, Sigma), glucose, aniline, ammonium peroxydisulfate (APS), hydrochloric acid, H_2PtCl_6, $NaBH_4$, N,N-dimethylformamide (DMF), ascorbic acid (AA), and uric acid (UA) were used as received. Nafion 117 solutions (0.5 wt %) were prepared by dilution with PBS (pH 6.5) of 5 wt % Nafion 117 solutions. All the chemicals were of analytical grade. Phosphate buffer solution (PBS, 0.2 M) was made up from H_3PO_4, Na_2HPO_4, and NaH_2PO_4. The glucose stock solution was allowed to mutarotate for at least 24 h before use. Deionized water was used throughout the experiments.

2.2. Synthesis of BNNTs-Pani-Pt-GOD Nanocomposites. Highly pure multiple BNNTs were synthesized using a high-frequency induction furnace by a carbon free chemical vapor deposition method, as elsewhere reported.[27] Generally speaking, the mixture of boron powder and FeO served as the precursor. The BNNTs were grown with an ammonia gas at high temperature. The as-grown BNNTs were further washed with HNO_3 in order to remove the remaining catalyst particles. The purified BNNTs have a pure white color appearance.

Five milligrams of BNNTs was dispersed in 5 mL of DMF by strong sonication over 1 h. Then, 20 mL of HCl (0.1 M) solution of aniline (1 mg mL^{-1}) was added with minimal agitation. After 5 min, 10 mL of APS solution (5 mg mL^{-1}) was added gently. The resulting solution was left undisturbed at the ambient temperature for a desirable time. Subsequently, the green-colored products were collected by filtering, thoroughly washed with water and ethanol thrice respectively, and finally dried under vacuum at room temperature. The final product was called BNNTs-Pani hybrids. The desired mass ratio of aniline to BNNTs is 4 to get optimized coverage of Pani on BNNTs and dispersibility of BNNTs-Pani hybrids.

Pt NPs were deposited on the surfaces of BNNTs-Pani hybrids as follows: 5 mg BNNTs-Pani hybrids and 200 μL 0.1 M H_2PtCl_6 were dispersed in 20 mL of deionized water by sonication. Then 10 mL of fresh aqueous solution containing 17.6 mg $NaBH_4$ was added. The reaction was carried out under magnetic stirring for 1 h at 60 °C. Finally, the precipitate was separated and rinsed with distilled water and ethanol three times, respectively. The precipitate was then dried in a vacuum oven at 60 °C overnight. The final product was a black powder and was called BNNTs-Pani-Pt. The desired mass ratio of Pt to BNNTs-Pani is 0.78.

Four mg BNNTs-Pani-Pt was dispersed in 2 mL of 0.2 M PBS (pH 6.5) with the aid of ultrasonic agitation to give a 2 mg mL^{-1} black suspension. GOD was also dissolved in 0.2 M PBS (pH 6.5) in another centrifuge tube at the same time and the concentration was 20 mg mL^{-1}. 60 μL BNNTs-Pani-Pt and 40 μL GOD were mixed with sonication for 10 min followed by incubation at 4 °C for at least 48 h. This suspension was called BNNTs-Pani-Pt-GOD nanobiocomposites liquid.

2.3. Fabrication of the Modified Electrodes. Glassy carbon (GC, 4.0 mm in diameter) electrode was polished with 1.0 and 0.3 μm alumina slurry sequentially and then washed ultrasonically in water and ethanol for a few minutes, respectively. The cleaned GC electrode was dried with a high-purify nitrogen steam for the next modification. Ten μL above-mentioned BNNTs-Pani-Pt-GOD nanobiocomposites suspension was spread evenly onto the GC electrode. Following closely 2 μL bovine serum albumin (BSA) and 2 μL of 1 wt % glutaraldehyde PBS solution (pH 6.5) were added and dried at room temperature for 2 h.

Scheme 1. Schematics of the Fabrication of BNNTs-Pani-Pt-GOD Nanobiocomposites

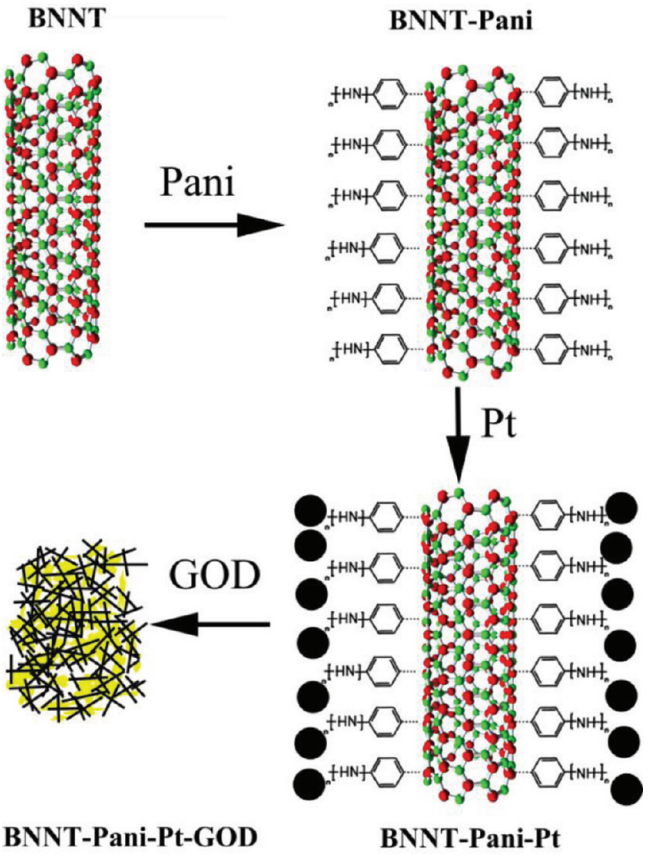

Finally, 4 μL of 0.5 wt % Nafion PBS (pH 6.5) solution was cast on the electrode to form a thin layer. This electrode was called GC/BNNTs-Pani-Pt-GOD. The as-prepared electrodes were stored in refrigerator (4 °C) when not in use.

2.4. Structural Characterization. As-prepared products were characterized by X-ray powder diffraction (XRD) with a Rigaku D/max-kA diffractometer with Cu Kα radiation (60 kV, 40 mA). UV−vis absorption spectra were collected with a TU-1901 spectrophotometer at room temperature. The morphology and components of the products were characterized using SU-70 high-resolution field-emission scanning electron microscopy (FESEM) and attached X-ray energy-dispersive spectrometry (EDS), respectively. The selected-area electron diffraction (SAED) patterns and high-resolution transmission electron microscopy (HRTEM) analyses were carried out on a Phillips Tecnai 20U-Twin high-resolution transmission electron microscope at an acceleration voltage of 200 kV. Raman spectrum was recorded using a Horiba Jobin-Yvon micro Raman spectrometer, equipped with a microscope and a 472.98 nm laser as the excitation source. The Fourier transform infrared (FTIR) spectra were recorded on a Bruker Tensor27 FTIR spectrometer using KBr pellets. The electrochemical tests were carried out on a PARSTAT 2273 electrochemical workstation consisting of a saturated calomel electrode (SCE) reference electrode, a platinum counter electrode, and a modified GC working electrode.

3. RESULTS AND DISCUSSION

3.1. Characterization of BNNTs-Pani Hybrids. The entire process for fabricating BNNTs-Pani-Pt-GOD nanobiocomposites is

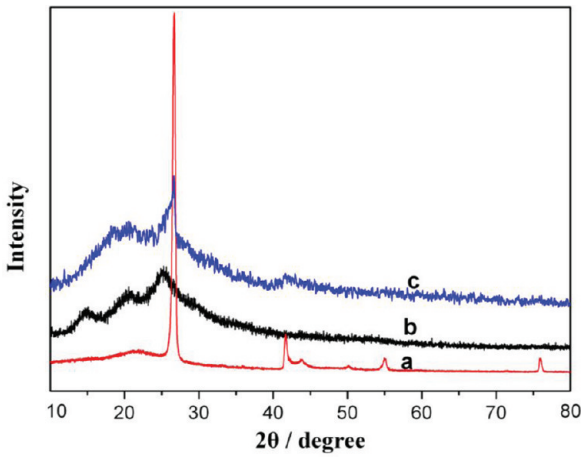

Figure 1. XRD pattern of (a) BNNTs, (b) Pani, and (c) BNNTs-Pani hybrids.

schematically shown in Scheme. 1. On the basis of large scale synthesis of BNNTs, the BNNTs were successfully modified and wrapped using polyaniline (Pani) to solve the water solubility. The water solubility of BNNTs paves the way for the following Pt loading. It is the key step for the Pt nanoparticle to homogeneously modify the water-soluble polyaniline-functionalized BNNTs for the amperometric glucose enzyme biosensor.

Figure 1 depicts XRD patterns of the BNNTs, Pani, and BNNTs-Pani hybrids. The diffraction peaks in curve a around 26, 42, and 55° can be, respectively, indexed to the (002), (100) and (004) planes of the hexagonal phase of BN with lattice parameters of a = 2.504 Å, c = 6.656 Å (h-BN, JCPDS card No. 34−0421). Curve b represents XRD pattern of Pani. As reported earlier,[28,29] in the XRD diffraction pattern, Pani shows broad peaks at 2θ of 15, 20.4, and 25.2°, corresponding to (011), (020), and (200) planes of Pani in its emeraldine salt form, respectively. The XRD pattern of the BNNTs-Pani (curve c) hybrids is interesting in the present work. The diffraction peak for Pani at 15° disappears and the peak at 25.2° for Pani can not be identified because of its overlapping with the (002) reflection of BNNTs. The peak at 20.4° splits into 3 peaks at 18.4, 20.6, and 23.6°, which indicates that the order of Pani chains changed in the presence of BNNTs. This can be explained that it exists strong $\pi-\pi$ interactions induced by broken symmetry between BNNTs and Pani.[16] Figure 2 shows the field-emission SEM images of the products. SEM image of as grown BNNTs is shown in Figure 2A. The product consists of straight nanowires with diameters of 50−80 nm and lengths of up to 10 μm. A typical SEM image of BNNTs-Pani hybrids is shown in Figure 2B. The synthesized hybrids display 1D nanostructures consisting of Pani shells and BNNT core nanostructures with enlarged diameters.

Figure 3A depcits Raman spectra of (a) BNNTs, (b) Pani and (c) BNNTs-Pani hybrids. The peak at 1362 cm^{-1} in Raman spectrum (curve a) corresponds to the counterphase BN vibrational mode (E_{2g}) within the BN sheets.[30] It is interesting that in the Raman spectrum of BNNTs-Pani hybrids, the BNNTs related peak shifts to 1351 cm^{-1}, whereas the Pani-related peak shifts to 1570 cm^{-1} from 1578 cm^{-1}. The BNNTs-related shift can be explained that the electronic structure of BNNTs can be modified by Pani wrapping. Meanwhile, the conformation change of Pani because of the interactions between BNNTs and Pani leads to the shift of Pani-related peak.[16]

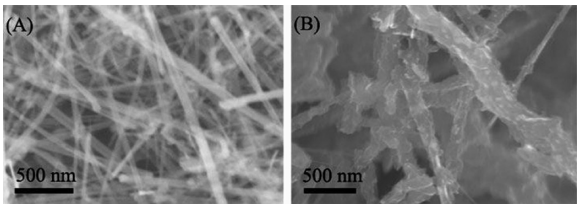

Figure 2. SEM images of (a) BNNTs and (b) BNNTs-Pani hybrids.

Figure 3B demonstrates comparative FT-IR spectra of BNNTs, Pani and BNNTs-Pani hybrids. Two strong vibrations at 810 and 1371 cm^{-1} (curve a), which are indexed to a B−N vibration perpendicular to and vibration along the tube axis respectively,[30] dominate the IR spectrum of BNNTs. In the IR spectrum of Pani (curve b), the peaks at 1550 and 1474 cm^{-1} belong to the C=C stretching of the quinoid ring and benzenoid ring, respectively. The peaks at 1293 and 1122 cm^{-1} are attributed to C−N stretching of the secondary aromatic amine. The peak at 790 cm^{-1} is ascribed to the out-of-plane bending of C−H on the 1,4-disubstituted ring. The peak at 1236 cm^{-1} can be attributed to various stretching and bending associated with the C−C bond. The strong band at 1122 cm^{-1} is a characteristic of conducting Pani.[23] It is surprising that in curve c, the B−N vibrations shift to 784 and 1364 cm^{-1} from 810 and 1371 cm^{-1}, respectively. Similar shifts can also be observed for Pani. The characteristic peak of conducting Pani shifts from 1122 to 1118 cm^{-1}, and the intensity is 4 times to that of origin Pani. This implies that π interactions take place between BNNTs and Pani located at N atoms from BNNTs and C atoms from Pani. This feature suggests that the BNNTs-Pani hybrids can be used as an electrode matrix for electrochemical investigation.

Figure 3C depicts the UV−vis spectrum of BNNTs, Pani and BNNTs-Pani hybrids, respectively. The curve b shows that pure Pani exhibits three absorption peaks at 356, 427, 800 nm, which are the characteristic absorption peaks of the emeraldine oxidation state of polyaniline.[31] The peak at 798 nm represents π-polaron transition indicating that Pani is in a conductive state.[32,33] After BNNTs were wrapped by Pani, the peak at 356 and 427 nm shift and overlap the paek at 280 nm. Importantly, another absorption peak appears at 815 nm (inset), which implies the wrapped Pani is still in a conductive state. For BNNTs, the strong absorption in the deep UV range with a maximum at 217 nm which corresponds to the optical bandgap of BNNTs[34] shifts to 207 nm in the composites. This shift implies that BNNTs may have a dopant effect, which was first mentioned by Zhi et. al.[16,35]

3.2. Characterization of BNNTs-Pani-Pt and BNNTs-Pani-Pt-GOD hybrids. TEM images for BNNTs-Pani-Pt composites are shown in Figure 4. The TEM images shown in Figure 4 A and B demonstrate that the surfaces of BNNTs-Pani hybrids are uniformly covered with a certain amount of Pt NPs with a mean diameter of ~5 nm, as shown in Figure 4D. The left down inset in Figure 4B is the selected area electron diffraction pattern (SAED), indicating the polycrystalline characteristic of the Pt nanocrystals. The (002) plane corresponding to hexagonal BN, while the (111), (200), and (220) planes correspond with Pt. Figure 4C shows a HRTEM lattice image of the Pt modified BNNTs-Pani hybrids. The lattice spacing of 0.23 nm marked in Figure 4C is in consistent with that of Pt (111) planes. Besides, 0.33 nm of the adjacent shells separation corresponds well with the d-spacing of (002) planes of BNNTs. Actually, the wrapped

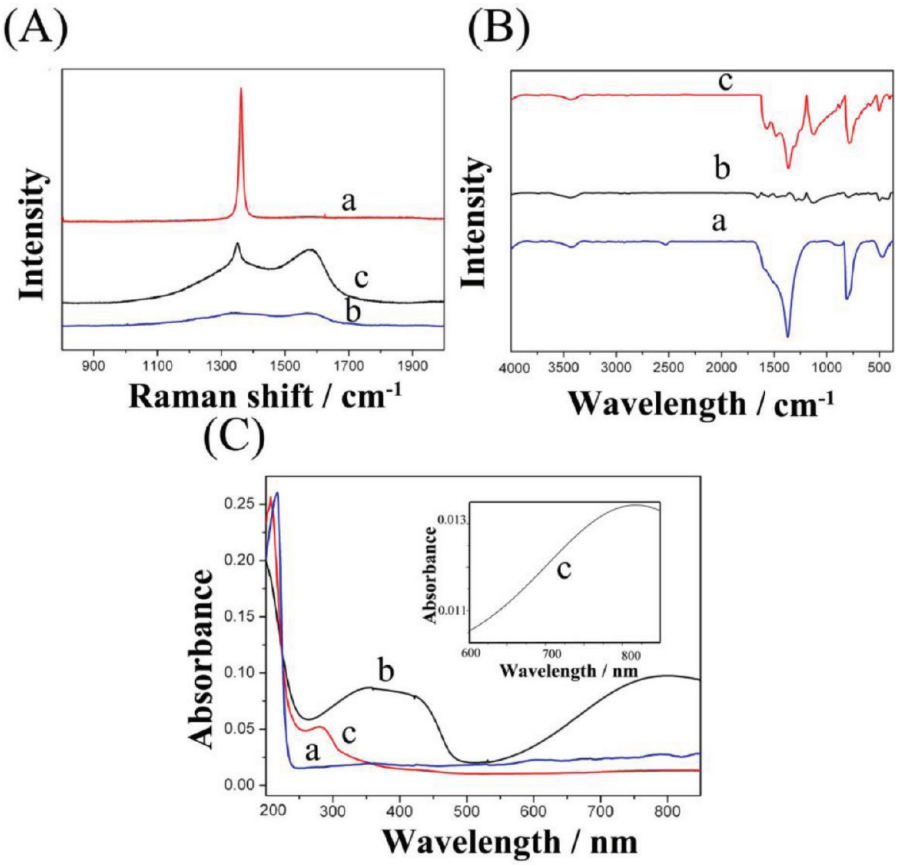

Figure 3. (A) Raman, (B) FT-IR, and (C) UV−vis absorption spectra of (a) BNNTs, (b) Pani, and (c) BNNTs-Pani hybrids.

Pani plays an important role for Pt loading. As previously reported, BNNTs are superhydrophobicity.[8,36] It is hard to load metal particles on the surface of BNNTs homogeneously directly, which is similar to CNTs.[37,38]

The BNNTs-Pani-Pt hybrids can be effectively used for the development of biosensors, glucose oxidase (GOD) was used as a model enzyme. The EDS mapping and UV−vis spectroscopy are used to examine whether the GOD can be immobilized in the BNNTs-Pani-Pt hybrids. After 48 h incubation, from SEM image in Figure 5A, it can be seen that the morphology of BNNTs-Pani-Pt-GOD is cotton-like. According to energy-dispersive X-ray spectroscopy (EDS) in Figure 5B, it is shown that the P element is presented in the EDS spectrum, indicating that GOD has been immobilized in BNNTs-Pani-Pt hybrids. The corresponding P mapping (Figure 5C) shows that P elements are homogenesouly distributed along the whole BNNTs-Pani-Pt-GOD hybrids. In addition, UV−vis spectroscopy was also used to detect the absorption band change of GOD in the BNNTs-Pani-Pt-GOD hybrids. In Figure 5D, curve a and b are the UV−vis spectra of GOD and BNNTs-Pani-Pt-GOD nanocomposites, respectively. GOD displays a sharp absorption peak at 229 and 276 nm along with a pair of peaks at 368 and 449 nm, corresponded to the oxidized form of flavin groups.[39] As seen from UV−vis spectra of BNNTs-Pani-Pt-GOD hybrids (curve b), the characteristic absorption peaks display no significant change in sites. However, it can be seen that the pair of peaks located at 368 and 449 nm are not well-defined compared to free GOD. This is probably due to some changes of the flavine cofactor from the active site of GOD. Also, the measurements in the aromatic region (250−320 nm) shows that the principal absorption peak of the BNNTs-Pani-Pt-GOD sample is retained at about 274 nm, a shift of ~2 nm toward lower wavelengths. It was reported by Tang et. al[40] that an electrostatic field around BN nanotube surfaces may be excited by intrinsic conformation. The same team also reported that protein such as glucose oxidase could be immobilized on the surfaces of BNNTs by the possible intrinsic electrostatic field.[13] We assume that GOD in the present work undergoes the similar process. The electrostatic field excited by BNNTs was not be shielded by Pani layer and have an effect on GOD.

3.3. Electrochemical Performance of the Prepared Electrodes. The electrochemical behavior of the GC/BNNTs-Pani-Pt-GOD electrode was investigated by cyclic voltammetry (CV) using $Fe(CN)_6^{3-/4-}$ as the redox marker in Figure 6A. The $Fe(CN)_6^{3-/4-}$ redox process is observed with a peak separation (ΔE_p) of about 80 mV, indicating a reversible electron transfer process. Compared with GC/BNNTs-Pani-Pt electrode, a decrease of peak current is obtained at the GC/BNNTs-Pani-Pt-GOD electrode, suggesting the bulk GOD molecules attached to the surface of the hybrids blocked the electron exchange between the redox probe and electrode surface. On the other hand, the peak currents of the $Fe(CN)_6^{3-/4-}$ redox process (anodic and cathodic) of the GC/BNNTs-Pani-Pt electrode are shown to be dependent on the scan rate (Figure 6B). The peak currents are linearly correlated to the square root of the scan rate in a range from 10 to 200 mV s^{-1} (inset of Figure 6B), implying that the electrochemical kinetics is a diffusion-controlled process.

Figure 7 shows the cyclic voltammograms obtained from the modified GC electrode with BNNTs-Pt, BNNTs-Pani and

BNNTs-Pani-Pt nanocomposites in 0.2 mM PBS solution in the absence and presence of 5 mM H_2O_2. As shown in Figure 7, the oxidation and reduction currents from H_2O_2 both at the BNNTs-Pt and BNNTs-Pani modified electrode are quite small, and the oxidation of H_2O_2 at the BNNTs-Pt modified electrode starts at 0.4 V. However, the electrochemical responses obtained at the GC/BNNTs-Pani-Pt are much larger than that obtained at the GC/BNNTs-Pt and GC/BNNTs-Pani electrodes. Moreover, it can be seen that the oxdation of H_2O_2 starts at 0.3 V, which is lower than that acquired at GC/BNNTs-Pt electrode. The decrease of the overpotential of H_2O_2 is ascribed to the electrocatalytic activity of the Pt NPs and Pani. It can be concluded that Pani and Pt NPs showed a synergistic effect on the electrocatalytic activity to H_2O_2.

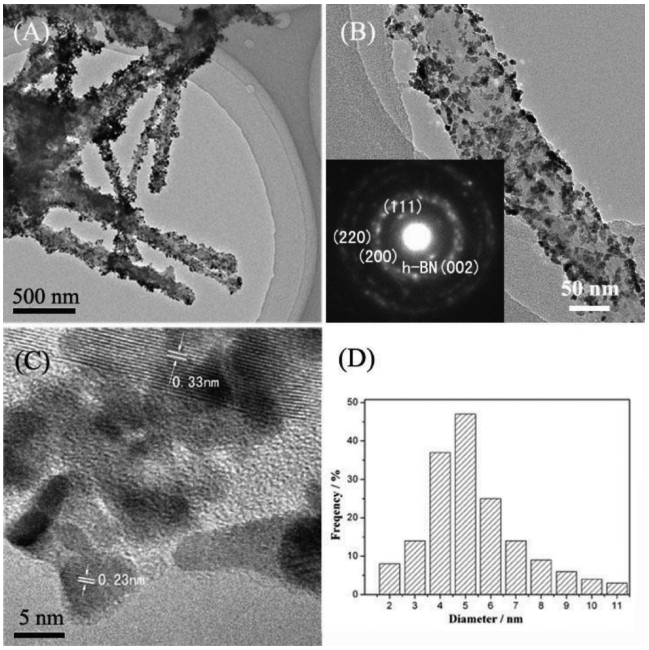

Figure 4. (A) Low-magnification TEM image of BNNTs-Pani hybrids modified with Pt nanoparticles. (B) TEM image of BNNTs-Pani hybrids covered with Pt nanoparticles, the inset is the corresponding electron diffraction pattern, the (002) plane corresponding to hexagonal BN, whereas the (111), (200), and (220) planes correspond with Pt. (C) High-resolution TEM image of a Pt modified BNNTs-Pani hybrid, the lattice spacing of 0.23 nm Figure 4C is in consistent well with that of Pt (111) planes, the lattice spacing of 0.33 nm corresponds well with the *d*-spacing of (002) planes of BNNTs. (D) Size distribution of Pt nanoparticles.

The portion of BNNTs-Pani-Pt to GOD with a mass ratio of 6/4 and the pH value of 6.5 PBS were selected for the amperometric detection of glucose. Figure 8A shows the amperometric response of the GC/BNNTs-Pani-Pt-GOD biosensor to the successive addition of glucose at room temperature. A response time of about 3 s (95% of steady-state current) is obtained. The response time is similar to that obtained by immobilizing GOD in polyaniline nanotubes (~3 s),[23] suggesting that the electrode responds rapidly to the change of glucose concentration. The electrode linearly responds to glucose at a lower concentration and attains a saturation level at a higher concentration as expected by Michaelis–Menten type enzyme kinetics as shown in Figure 8B. An apparent Michaelis–Menten constant of 3.4 mM is estimated from the Lineweaver–Burke plot of the calibration data. The response current for glucose detection at the GC/BNNTs-Pani-Pt-GOD electrode increases linearly from 0.01 to 5.5 mM glucose, and reaches a saturation sate at about 13 mM. The sensitivity of detection is estimated to be 19.02 mA M^{-1} cm^{-2}, similar to that of Au NPs-Pani glucose sensor[41] and higher than that of Pt-CNT nanocomposite glucose sensor.[42] The detection limit is estimated to be about 6 μM for a signal-to-noise of 3. The relative standard deviation (RSD) of the bioenzyme biosensor for replicate measurements of 0.5 mM glucose is 3.7% at 5 different biosensors.

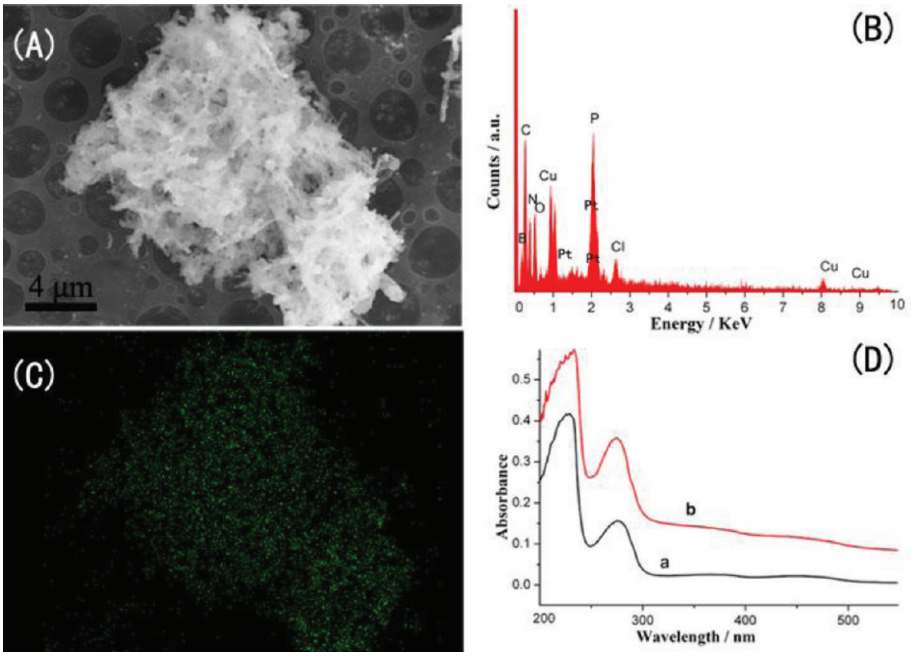

Figure 5. (A) SEM image of BNNTs-Pani-Pt-GOD composites and (B) the corresponding EDS spectrum. (C) P map of the composites. (D) UV–vis spectrum of (a) pure GOD and (b) BNNTs-Pani-Pt-GOD in aqueous solution.

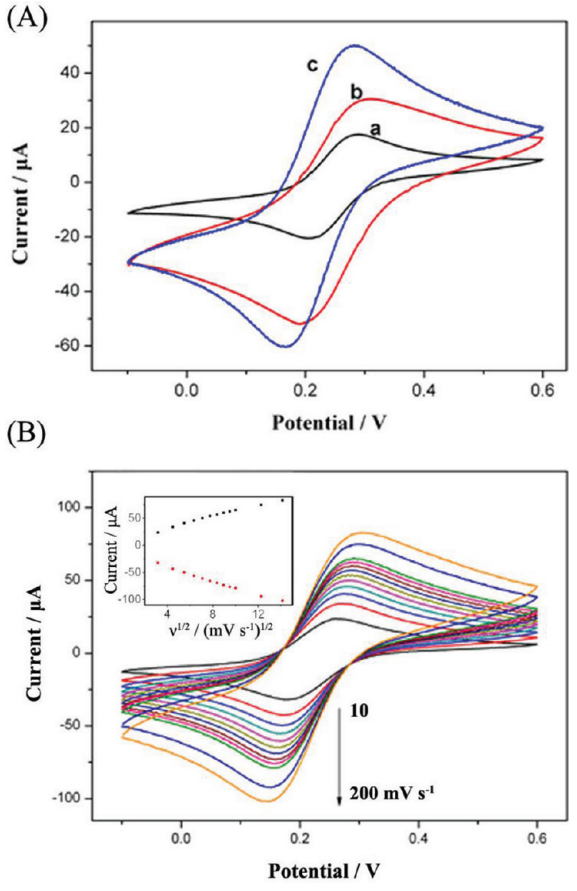

Figure 6. (A) Cyclic voltammograms of (a) GC, (b) GC/BNNTs-Pani-Pt, (c) GC/BNNTs-Pani-Pt-GOD electrodes for 1 mM potassium ferricyanide containg 0.2 M KNO_3 at 50 mV S^{1-}. (B) Cyclic voltammograms of the GC/BNNTs-Pani-Pt electrode at scan rates of 10, 20, 30, 40, 50, 60, 70, 80, 90, 100, 150, and 200 mV s^{-1} in 1 mM PBS (pH 6.5) of $Fe(CN)_6^{3-/4-}$ containg 0.2 M KNO_3.

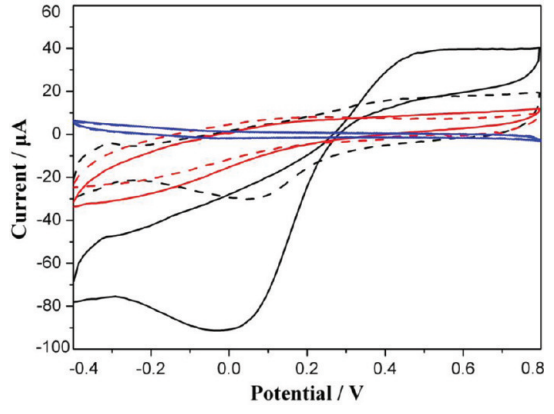

Figure 7. Cyclic voltammograms of GC/BNNTs-Pt (red) GC/BNNTs-Pani (blue)and GC/BNNTs-Pani-Pt (black) electrodes obtained in the absence (dotted line) and presence (solid line) of 5 mM H_2O_2 in 0.2 mM PBS solution at 50 mV s^{-1} (vs SCE).

Table 1 gives a comparison of the analytical performance characteristics for recent reports Pt—based enzyme glucose biosensor. It can be seen that the presented glucose biosensor

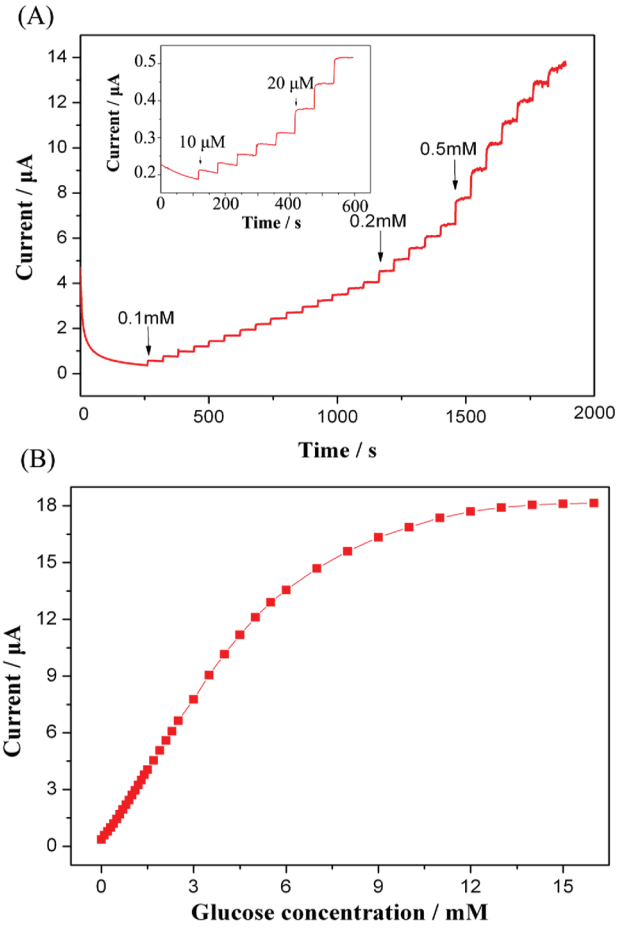

Figure 8. (A) Amperometric response for GC/BNNTs-Pani-Pt-GOD electrode upon successive addition of glucose in 0.2 M PBS (pH 6.5) at an applied potential of 0.55 V. The inset in A is amperometric response to the sequential addition of 10 μM and 20 μM glucose. (B) Calibration curve for glucose concentrations at the GC/BNNTs-Pani-Pt-GOD electrode (vs SCE).

exhibited good performance with wide linear range, high sensitivity and low detection limit.

In real physiological samples, the electroactive compounds such as ascorbic acid (AA) and uric acid (UA) usually cause problems in the accurate determination of glucose. In the present experiment, the current signals generated by adding 0.1 mM AA and UA were negligible compared with that of 1 mM glucose. This can be contributed to the negatively charged Nafion which is permselective barrier to repel electroactive interferences.[48] This make the proposed biosensor be used in practical applications.

To reveal the effect of BNNTs on the enzymatic activity of GOD, the pH stability of the biosensors was evaluated. The appropriate pH was adjusted by using 0.2 M phosphoric acid. As shown in Figure 9, with the pH value of the supported electrolyte increasing, the activity of GC/Pani-Pt-GOD electrode increases and reaches the maximum at pH 6.5. Surprisingly, for the GC/BNNTs-Pani-Pt-GOD electrode, the relative activity keeps almost no change in the range from pH 3 to 7. Figure 10A shows a study of acid deactivation of GC/BNNTs-Pani-Pt-GOD electrode by dipping in acidic solution with different pH values. This glucose sensor retains its activity after it is dipped in acidic solutions of pH value higher than 2.0 for 60 min. With the pH

Table 1. Comparison of Analytical Performance of Some Pt-Based Enzyme Glucose Biosensors

electrode	linearity (mM)	sensitivity (mA M^{-1} cm^{-2})	detection limit (μM)	authors
GOD/Pt/FGS/chitosan/GCE	sub 0.001−5	117.89	0.6	Hong et.al.[43]
(GOx)/BSA/PtNP-SWCNT	0.04−0.87	4.54	40	Zeng et al.[44]
MSN−PtNP−GOx	0.001−26	4.35	0.8	Li et al.[45]
MS/Pt-DENs/GOx	0.02−10	15.7	4	Han et al.[46]
GOD/Pt/OMC/Au	0.05−3.7	12	50	Jiang et al.[47]
BNNTs-Pani-Pt-GOD	0.01−5.5	19.02	6	this work

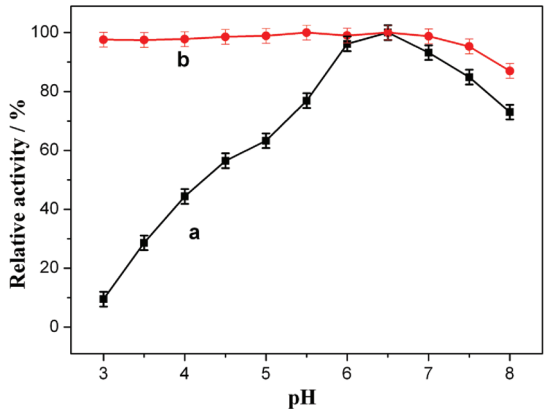

Figure 9. Effect of solution pH values on the amperometric responses of 0.3 mM glucose in 0.2 M PBS at (a) the Pani-Pt-GOD and (b) BNNTs-Pani-Pt-GOD nanocomposites modified glassy carbon electrode at a working potential of +0.55 V (vs SCE).

values decreasing, a slow decay of its current signal is observed between pH 2.0 and 3.0. When the pH values are less than 2.0, this decay of the glucose sensor gets faster. Figure 10B displays the influence of the immersion time in acidic media pH 2.0 upon the response of the GOD enzyme electrode. The biosensor still retains its 25% original response activity even after a 180 min acid incubation, displaying the high stability of GC/BNNTs-Pani-Pt-GOD glucose biosensor.

The exact reason for the resistance to acid-induced denaturation provided by BNNTs is not fully understood, some interpretations of this unusual observation will be raised. On one side, immobilized GOD molecules via electrostatic absorption have restricted mobility, which prevents the structural change and retain enzymatic activity. On the other hand, much similar to carbon pasted enzyme electrodes[49] and colloidal gold-modified carbon ionic liquid enzyme electrode[39] reported eleswhere, the hydrophobic BNNTs can play a role as a barrier to hydronium ions. This lead to the retention of the ionization state of the protein ionogenic groups of enzymes like glucose oxidase.

The effect of temperature on the relative activities of GC/Pani-Pt-GOD and GC/BNNTs-Pani-Pt-GOD biosensors was also investigated. (Figure 11). The tendency of the activity of GC/BNNTs-Pani-Pt-GOD is interesting. When the temperature is less than 35 °C, it seems that the activity is partially locked compared with GC/Pani-Pt-GOD electrode. With the temperature increasing, the activity increases until 60 °C. It should be

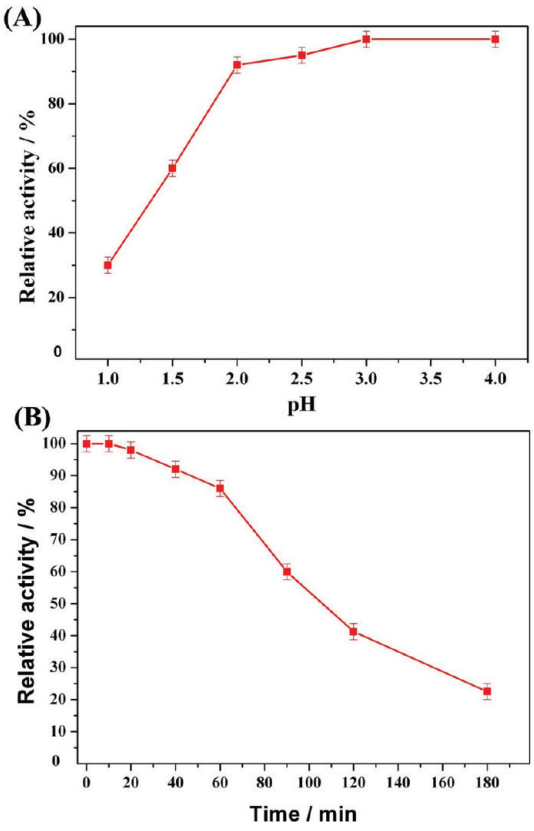

Figure 10. (A) Influence of the pH value on the enzymatic activity of GC/BNNTs-Pani-Pt-GOD. (B) Deactivation kinetics at pH 2.0 of GC/BNNTs-Pani-Pt-GOD biosenser. The activity was recorded at times indicated using amperometric monitoring of 0.3 mM glucose, applied potential: +0.55 V (vs SCE).

noted that this temperature to retain enough GOD enzymatic activity is pretty high in comparison with GC/Pani-Pt-GOD (40 °C) and previous works reported.[23,26,50] It is believed that the high GOD enzymatic activity of the GC/BNNTs-Pani-Pt-GOD biosnesor at high temperature is attributed to the effect of BNNTs. The interactions between BNNTs and GOD as mentioned above might reduce the conformational flexibility and result in higher activation energy for the enzyme molecule to reorganize its proper conformation.[50,51] Of course, the related mechanism needs to be investigated further. The stability of the biosensor was also investigated under storage conditions of pH 6.5 in PBS solution at 4 °C. The current response for 0.3 mM glucose was measured everyday. Up to 40 days, the current response still kept above 95% of its original response.

4. CONCLUSIONS

A new type of amperometric biosensor, based on the BNNTs-Pani-Pt hybrids with Pt nanoparticle decorated on polyaniline (Pani)-wrapped boron nitride nanotubes (BNNTs), is presented in this article. The microstructure and chemical bonding state of the Pt modified Pani-wrapped BNNTs hybrids were systematically investigated using Raman spectra, Fourier transform infrared (FTIR) spectra, UV−vis spectra, X-ray energy-dispersive spectroscopy, field-emission electron microscopy, transmission electron microscopy, and X-ray diffraction pattern. It is shown that π interactions take place between BNNTs and polyaniline (Pani)

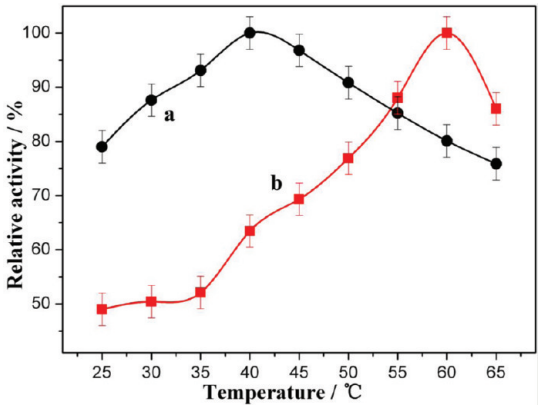

Figure 11. Contrastive study of the effect of temperature on the activities of (a) GC/Pani-Pt-GOD and (b) GC/BNNTs-Pani-Pt-GOD electrodes.

located at N atoms from BNNTs and C atoms from Pani, resulting in water solubility of the Pani wrapped BNNTs hybrids. It is the key step for the Pt nanoparticle to homogeneously modify the water-soluble Pani-functionalized BNNTs for the development of the amperometric glucose enzyme biosensor. The glucose oxidase can be successfully immobilized in BNNTs-Pani-Pt hybrids. The resulting amperometric glucose biosensor based on the BNNTs-Pani-Pt hybrids exhibited a fast response time (within 3 s) and a linear calibration range from 0.01 to 5.5 mM with a high sensitivity and low detection limit of 19.02 mA M^{-1} cm^{-2} and 0.18 μM glucose (S/N = 3). The developed biosensor exhibited excellent acid stability and heat resistance. Surprisedly, the relative activity of GC/BNNTs-Pani-Pt-GOD electrode keeps almost no change in the range from pH 3 to 7. When the temperature is less than 35 °C, it seem that the activity is partially locked. With the temperature increasing, the activity increases until 60 °C. We owe this to the effect of electrostatic field and hydrophobia of BNNTs. The GC/BNNTs-Pani-Pt hybrid biosensors would open new horizons for fabrication of biosensors and biocatalysts.

AUTHOR INFORMATION

Corresponding Author

*Tel.: + 86 531 88396970. Fax: + 86 531 88396970. E-mail: yinlw@sdu.edu.cn.

ACKNOWLEDGMENT

We acknowledge support from the National Natural Science Funds for Distinguished Young Scholars (51025211), National Nature Science Foundation of China (Nos.50872071 and 50972079), the Shandong Natural Science Fund for Distinguished Young Scholars (JQ200915), the Nature Science Foundation of Shandong Province (Y2007F03 and Y2008F26), the Foundation of Outstanding Young Scientists in Shandong Province (2006BS04030), the Tai Shan Scholar Foundation of Shandong Province, and the Gong Guan Foundation of Shandong Province (2008GG10003019).

REFERENCES

(1) Chopra, N. G.; Luyken, R. J.; Cherrey, K.; Crespi, V. H.; Cohen, M. L.; Louie, S. G.; Zettl, A. *Science* **1995**, *269*, 966–967.
(2) Zhi, C. Y.; Bando, Y.; Tang, C. C.; Xie, R. G.; Sekiguchi, T.; Golberg, D. *J. Am. Chem. Soc.* **2005**, *127*, 15996–15997.
(3) Li, C.; Bando, Y.; Zhi, C. Y.; Huang, Y.; Golberg, D. *Nanotechnology* **2009**, *20*, 385707.
(4) Yin, L. W.; Bando, Y.; Golberg, D.; Gloter, A.; Li, M. S.; Yuan, X. L.; Sekiguchi, T. *J. Am. Chem. Soc.* **2005**, *127*, 16354–16355.
(5) Terao, T.; Bando, Y.; Mitome, M.; Zhi, C. Y.; Tang, C. C.; Golberg, D. *J. Phys. Chem. C* **2009**, *113*, 13605–13609.
(6) Wen, Z. H.; Ci, S. Q.; Li, J. H. *J. Phys. Chem. C* **2009**, *113*, 13482–13487.
(7) Lin, Y. H.; Lu, F.; Tu, Y.; Ren, Z. F. *Nano Lett.* **2004**, *4*, 191–195.
(8) Li, L. H.; Chen, Y. *Langmuir.* **2010**, *26*, 5135–5140.
(9) Doris, E.; Maguer, A.; Leroy, E.; Bresson, L.; Loiseau, A.; Mioskowski, C. *J. Mater. Chem.* **2009**, *19*, 1271–1275.
(10) Rao, C. N. R.; Pal, S.; Vivekchand, S. R. C.; Govindaraj, A. *J. Mater. Chem.* **2007**, *17*, 450–452.
(11) Zhi, C.; Bando, Y.; Wang, W.; Tang, C.; Kuwahara, H.; Golberg, D. *Chem.—Asian J.* **2007**, *2*, 1581–1585.
(12) Gao, Z. H.; Zhi, C. Y.; Bando, Y.; Golberg, D.; Serizawa, T. *ACS Appl. Mater. Interfaces* **2011**, *3*, 627–632.
(13) Zhi, C.; Bando, Y.; Tang, C.; Golberg, D. *J. Am. Chem. Soc.* **2005**, *127*, 17144–17145.
(14) Wang, W. L.; Bando, Y.; Zhi, C. Y.; Fu, W. Y.; Wang, E. G.; Golberg, D. *J. Am. Chem. Soc.* **2008**, *130*, 8144–8145.
(15) Sun, Y. P.; Xie, S. Y.; Wang, W.; Fernando, K. A. S.; Wang, X.; Lin, Y. *Chem. Commun.* **2005**, 3670–3672.
(16) Zhi, C. Y.; Bando, Y.; Tang, C. C.; Honda, S.; Sato, K.; Kuwahara, H.; Golberg, D. *Angew. Chem., Int. Ed.* **2005**, *44*, 7929–7932.
(17) Velayudham, S.; Lee, C. H.; Xie, M.; Blair, D.; Bauman, N.; Yap, Y. K.; Green, S. A.; Liu, H. Y. *ACS Appl. Mater. Interfaces* **2010**, *2*, 104–110.
(18) Mi, H.; Zhang, X.; Yang, S.; Ye, X.; Luo, J. *Mater. Chem. Phys.* **2008**, *112*, 127–131.
(19) Wang, J.; Torardi, C. C.; Duch, M. W. *Synth. Met.* **2007**, *157*, 851–859.
(20) Hou, L.; Hou, Q.; Mo, Y.; Peng, J.; Cao, Y. *Appl. Phys. Lett.* **2005**, *87*, 243504–243506.
(21) Martin, C. R. *Acc. Chem. Res.* **1995**, *28*, 61–68.
(22) Liu, H.; Kameoka, J.; Czaplewski, D. A.; Craighead, H. G. *Nano Lett.* **2004**, *4*, 671–675.
(23) Wang, Z. Y.; Liu, S. N.; Wu, P.; Cai, C. X. *Anal. Chem.* **2009**, *81*, 1638–1645.
(24) Gvozdenovic, M. M.; Jugovic, B. Z.; Bezbradica, D. I.; Antov, M. G.; Knezevic-Jugovic, Z. D.; Grgur, B. N. *Food Chem.* **2011**, *124*, 396–400.
(25) Wan, D.; Yuan, S. J.; Li, G. L.; Neoh, K. G.; Kang, E. T. *ACS Appl. Mater. Interfaces* **2010**, *2*, 3083–3091.
(26) Zhou, H. H.; Chen, H.; Luo, S. L.; Chen, J. H.; Wei, W. Z.; Kuang, Y. F. *Biosens. Bioelectron.* **2005**, *20*, 1305–1311.
(27) Zhi, C. Y.; Bando, Y.; Tan, C. C.; Golberg, D. *Solid State Commun.* **2005**, *135*, 67–70.
(28) Ghatak, S.; Chakraborty, G.; Meikap, A. K.; Woods, T.; Babu, R.; Blau, W. J. *J. Appl. Polym. Sci.* **2011**, *119*, 1016–1025.
(29) Yan, J.; Wei, T.; Fan, Z. J.; Qian, W. Z.; Zhang, M. L.; Shen, X. D.; Wei, F. *J. Power Sources* **2010**, *195*, 3041–3045.
(30) Zhi, C. Y.; Bando, Y.; Tang, C. C.; Golberg, D.; Xie, R. G.; Sekigushi, T. *Appl. Phys. Lett.* **2005**, *86*, 213110–213114.
(31) Jana, T.; Nandi, A. K. *Langmuir.* **2000**, *16*, 3141–3147.
(32) Athawale, A. A.; Kulkarni, M. V.; Chabukswar, V. V. *Mater. Chem. Phys.* **2002**, *73*, 106–110.
(33) Jafarzadeh, S.; Thormann, E.; Ronnevall, T.; Adhikari, A.; Sundell, P. E.; Pan, J. S.; Claesson, P. M. *ACS Appl. Mater. Interfaces* **2011**, *3*, 1681–1691.
(34) Lee, C. H.; Wang, J. S.; Kayatsha, V. K.; Huang, J. Y.; Yap, Y. K. *Nanotechnology* **2008**, *19*, 455605.
(35) Zhi, C. Y.; Zhang, L. J.; Bando, Y.; Terao, T.; Tang, C. C.; Kuwahara, H.; Golberg, D. *J. Phys. Chem. C* **2008**, *112*, 17592–17595.
(36) Lee, C. H.; Drelich, J.; Yap, Y. K. *Langmuir.* **2009**, *25*, 4853–4860.
(37) Wu, H. X.; Cao, W. M.; Li, Y.; Liu, G.; Wen, Y.; Yang, H. F.; Yang, S. P. *Electrochim. Acta* **2010**, *55*, 3734–3740.

(38) Jiang, H.; Zhu, L.; Moon, K.-S.; Wong, C. P. *Carbon* **2007**, *43*, 655–661.
(39) Stoscheck, C. M. *Method. Enzymol.* **1990**, *182*, 50–68.
(40) Tang, C. C.; Li, J. G.; Bando, Y.; Zhi, C. Y.; Golberg, D. *Chem.-Asian J* **2010**, *5*, 1220–1224.
(41) Xian, Y. Z.; Hu, Y.; Liu, F.; Xian, Y.; Wang, H. T.; Jin, L. T. *Biosens. Bioelectron.* **2006**, *21*, 1996–2000.
(42) Wen, D.; Zou, X. Q.; Liu, Y.; Shang, L.; Dong, S. J. *Talanta* **2009**, *79*, 1233–1237.
(43) Lin, Y. H.; Wu, H.; Wang, J.; Kang, X. H.; Wang, C. M.; Wang, D. H.; Liu, J.; Aksay, I. A. *Talanta* **2009**, *80*, 403–406.
(44) Zhang, H.; Zeng, Z. Y.; Zhou, X. Z.; Huang, X. A.; Wang, Z. J.; Yang, Y. L.; Zhang, Q. C.; Boey, F. *Analyst.* **2010**, *135*, 1726–1730.
(45) Li, H. L.; He, H.; Zhao, J.; Wu, Y. F.; Cai, D.; Wei, Y. Y.; Yang, Q. *Electrochim. Acta* **2011**, *56*, 2960–2965.
(46) Zhu, Y. H.; Han, X. A.; Yang, X. L.; Zhang, J. M.; Li, C. Z. *J. Solid-State Electrochem.* **2011**, *15*, 511–517.
(47) Zhu, L. D.; Jiang, X. Y.; Wu, Y. H.; Mao, X. Y.; Cui, X. J. *Sens. Actuators, B* **2011**, *153*, 158–163.
(48) Burmeister, J. J.; Gerhardt, G. A. *Anal. Chem.* **2001**, *73*, 1037–1042.
(49) Wang, J.; Musameh, M.; Mo, J. W. *Anal. Chem.* **2006**, *78*, 7044–7047.
(50) Bayramoglu, G.; Metin, A. U.; Altintas, B.; Arica, M. Y. *Bioresour. Technol.* **2010**, *101*, 6881–6887.
(51) Bayramoglu, G.; Kaya, B.; Arica, M. Y. *Food Chem.* **2005**, *92*, 261–268.